Nucleic Acids Research, 1996, Vol. 24, No. 24 **4969–4977**

In vivo generation of 3′ and 5′ truncated species in the process of c-*myc* mRNA decay

Panayotis Ioannidis[1,2], Maria Havredaki[1], Nelly Courtis[2] and Theoni Trangas[2,*]

[1]Institute of Biology, NCSR–Demokritos, Athens, Greece and [2]Papanikolaou Research Center of Oncology, 'St Savvas' Hospital, 171 Alexandras Avenue, 11522 Athens, Greece

Received August 12, 1996; Revised and Accepted November 8, 1996

ABSTRACT

It has been demonstrated that the half-life of c-*myc* mRNA is modulated in response to physiological agents. The elucidation of the decay process and the identification of the critical steps in the *in vivo* c-*myc* mRNA degradation pathway can be approached by following the fate of c-*myc* mRNA under the influence of such factors. IFN-α was the factor used to modulate c-*myc* mRNA half-life in HeLa 1C5 cells, a stable clone derived from HeLa cells. This cell line carries multiple copies of the c-*myc* gene, under the control of the dexamethasone inducible mouse mammary tumor virus-long terminal repeat (MMTV-LTR). Exposure of HeLa 1C5 cells to IFN-α resulted in a further 2-fold increase over the dexamethasone-induced c-*myc* mRNA. However, the c-*myc* mRNA in IFN-α treated cells was less stable than that in the control cells. RNase H mapping of the 3′ untranslated region of c-*myc* mRNA revealed, in addition to the full length mRNA, three smaller fragments. These fragments were proven to be truncated, non-adenylated c-*myc* mRNA species generated *in vivo.* Exposure of HeLa 1C5 cells to Interferon-α before induction with dexamethasone resulted in the enhanced presence of these intermediates. RNase H analysis of c-*myc* mRNA after actinomycin D chase revealed that deadenylation led to the formation of a relatively more stable oligoadenylated c-*myc* mRNA population which did not appear to be precursor to the truncated intermediates. The detection of truncated 3′ end c-*myc* mRNA adenylated fragments as well, implies that the c-*myc* mRNA degradation process may follow an alternative pathway possibly involving endonucleolytic cleavage.

INTRODUCTION

The activation of c-*myc* protooncogene is implicated in tumorigenesis and is attributed to such diverse mechanisms as amplification, translocation, promoter insertion or retroviral transduction. All the above result in the constitutive expression of the gene which is implicated in oncogenesis *in vivo* and *in vitro* (for reviews see 1 and 2). Recently it has become clear that c-*myc* also serves pleiotropic cellular functions. Apart from its role as a factor controlling cellular proliferation, it also plays a central role in programmed cell death (apoptosis) (3,4). *MYC* proteins are nuclear phosphoproteins with helix–loop–helix leucine zipper domains specifying DNA and protein–protein interactions. *MYC* forms heterodimers with Max protein and acts as a transcription factor (reviewed in 5).

A complex array of regulatory mechanisms is involved in c-*myc* expression, including both transcriptional and post-transcriptional processes (1,2). The rapid downregulation of the gene is made possible by the instability of the corresponding mRNA (6) and protein products (7). Alterations of the half-life of c-*myc* mRNA have been documented and have been proven to be pivotal for c-*myc* gene expression. Modulation of the half-life of c-*myc* mRNA provides a commonly observed mechanism of c-*myc* regulation, often superimposed on transcriptional control. For example, mitogen stimulation of G_0 arrested fibroblasts (8) resulted in increased half-life of the mRNA. On the other hand, induction of differentiation of MEL (9) and HL-60 (10) cells causes a decrease in the half-life of c-*myc* mRNA. Primary structure alterations of c-*myc* mRNA which result in lengthened half-life are often responsible for the deregulated c-*myc* expression in tumors (reviewed in 11).

Given the importance of mRNA stability in the regulation of gene expression, in a number of genes which also include other oncogenes, cytokines, interferons and growth factors, understanding the mechanisms underlying the control of RNA decay is important. One approach is to define RNA domains which can destabilize mRNA and are characteristic of short-lived mRNAs. Shaw and Kamen (12) observed that many transiently expressed mRNAs including GM-CSF, c-*fos* and c-*myc* have (A+U)-rich sequences (AREs) in their 3′ untranslated region (UTR), which often contain multiple copies of the sequence with the core motif AUUUA. Construction of chimeric mRNAs containing such sequences at the 3′ end of the stable globin mRNA resulted in the rapid decay of the message. The short half-life of c-*myc* is attributed to 3′ UTR sequences which contain two copies of the AUUUA motif. Fusion of c-*myc* 3′ UTR to the relatively stable neo mRNA resulted in reduction of the half-life from 6 h to 45 min (13). It has been proposed that certain other segments in addition to AUUUA in the 3′ UTR region may contribute to the rapid decay of this message (14). Proteins which recognize specific sequences in this region have been identified and their role in modifying mRNA stability is under investigation (15–17). In addition to the instability determinant found within the 3′ UTR, c-*myc* mRNA also contains a sequence within the region coding for 335–439 amino acids that contributes to the rapid decay of

*To whom correspondence should be addressed. Tel: +30 1 6437210/6409466; Fax: +30 1 6421022/6420146; Email: t.trangas@genet.ath.forthnet.gr

c-*myc* mRNA. These coding sequences transferred to chimeric constructs conferred instability, independently of the presence of the 3′ UTR elements. The destabilizing role of this element depends on c-*myc* translation (18).

Mechanisms of degradation of unstable mRNAs (c-*fos*, c-*myc*) have been studied by both *in vivo* and *in vitro* approaches. The available data demonstrate a sequential pathway in which deadenylation precedes degradation of the main body of the mRNA (11). The removal of the poly(A) tail in unstable mRNAs is very rapid as supposedly is the removal of the final adenosine residues. In contrast, in stable mRNAs, deadenylation is delayed upon reaching the last 30–60 adenosine residues. The failure to identify intermediate products in unstable mRNAs led to the assumption that following deadenylation, the main body of mRNA is degraded very rapidly by exonucleolytic cleavage.

In order to elucidate the critical steps in the c-*myc* decay pathway, we used a different approach. Our goal was to detect alterations in the decay process under conditions in which the half-life of c-*myc* mRNA is modulated. Among the factors known to affect c-*myc* mRNA stability *in vivo* are interferons (IFNs). Several lines of evidence suggest that IFNs act as negative regulators of c-*myc* expression in certain cell systems. IFNs have been shown to decrease the steady state levels of c-*myc* mRNA in Daudi cells and in murine sarcoma virus transformed NIH 3T3 cells. In the Daudi lymphoblastoma cells, IFN-α and IFN-β have been shown to decrease the levels of c-*myc* transcripts via a postranscriptional mechanism, i.e., by selectively increasing the rate of degradation of c-*myc* mRNA (19,20). Based on the available data about c-*myc* mRNA mechanism of degradation, it may be possible that IFNs act by either preventing the formation of long poly(A) tails or by accelerating the deadenylation process. It is also possible that IFN-α may utilize an other mechanism to exert its destabilizing action.

The system used in this study was a clone derived from HeLa cells transfected with a dexamethasone (DX) inducible c-*myc* expression vector. Exposure of these cells to IFN-α resulted in the overexpression of c-*myc* mRNA which nevertheless, decayed faster than that of the control cells. Using this system, which provided high levels of c-*myc* expression, we have been able to identify specific degradation intermediates of c-*myc* mRNA generated *in vivo*: (i) a distinct population of c-*myc* mRNA with shortened poly(A) tails derived through deadenylation and (ii) truncated c-*myc* mRNA species lacking 3′ end sequences. The detection of adenylated truncated fragments as well, indicated that c-*myc* mRNA degradation may involve endonucleolytic cleavage.

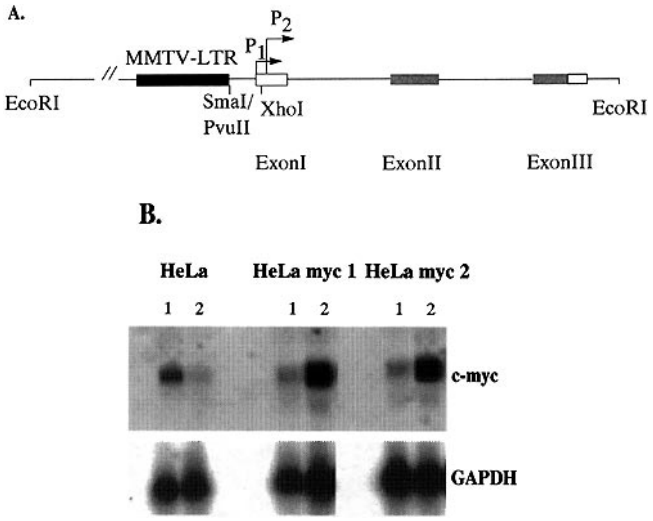

Figure 1. (**A**) Schematic representation of the pMSG-*myc* vector. c-*myc* genomic sequences were cloned into the pMSG vector as described under Materials and Methods. The positions of the restriction sites used in cloning are indicated on the diagram. P1 and P2 indicate the positions of the c-*myc* promoters. Open and grey boxes represent non-coding and coding regions respectively. (**B**) Dexamethasone induction of c-*myc* mRNA transcription in transfected cells and downregulation of this message in the parental cell line. c-*myc* mRNA expression in HeLa cells and in two pools of transfected cell populations (HeLa myc-1 and HeLa myc-2) after addition of 10% FCS (lane 1) and 10% FCS plus 3×10^{-7} M DX (lane 2) for 2 h. Expression of the unregulated gene GAPDH confirmed that similar amounts of total cellular RNA were added per lane.

MATERIALS AND METHODS

Vector construction and cell transfection

Human genomic c-*myc* DNA (from pHSR-1 plasmid, American Type Culture Collection) was inserted 3′ to MMTV-LTR into pMSG eukaryotic expression vector (Pharmacia), in two steps. First, *Pvu*II–*Xho*I c-*myc* DNA fragment (–353 to +66 relative to P1 promoter) was ligated to *Sma*I and *Xho*I sites into the polylinker of pMSG. Consequently, *Xho*I–*Eco*RI (ending 500 bp 3′ to pA2 polyadenylation sequences) c-*myc* genomic DNA fragment was ligated to the above construct. This ligation resulted to the excision of the SV40 polyadenylation signal sequences of the vector so that polyadenylation of c-*myc* mRNA would be controlled by its own signals (Fig. 1A). c-*myc* nucleotide sequences given throughout this paper refer to the sequence published by Gazin *et al.* (21).

HeLa cells were grown in RPMI 1640 supplemented with 10% FCS. Prior to transfection, HeLa cells were cultured for three passages in DMEM containing 10 mM HEPES and 10% FCS.

Transfection of HeLa cells was performed by the calcium phosphate precipitation method. 5×10^5 cells per 25 cm^2 flask were seeded and cultured overnight in DMEM with HEPES and 10% FCS. Medium was changed 4 h prior to transfection and cotransfection was performed with pMSG-*myc* and pSV2-neo as described by Graham *et al.* (22), without using carrier DNA. After 24 h of exposure to DNA precipitate and a further 24 h incubation in fresh medium, G418 (400 μg/ml) (Gibco-BRL) selection was applied for 22 days. Individual colonies were isolated, grown in mass cultures and analysed by Southern blot hybridization.

Cell culture

HeLa 1C5 cells were cultured and maintained in RPMI 1640 with 10% FCS in the continuous presence of 300 μg/ml G418. Prior to each experiment cells were cultured for 48 h in RPMI 1640 plus 10% FCS and subsequently in fresh medium with 0.25% FCS for 48 h, before the addition of fresh RPMI 1640 containing 10% FCS or 10% FCS plus 10^{-5} M dexamethasone (induction). Exposure to IFN-α was performed by addition of 200 U/ml, 24 h before induction.

Northern hybridization

Total RNA was isolated as described by Chomczynski and Sacchi (23). An aliquot of 30 µg of denatured total RNA was electrophoresed in 1.2% formaldehyde–agarose gels, transferred to nylon membranes (Zetaprobe, BioRad), immobilized and hybridized according to the manufacturer's instructions.

c-*myc* (1.3 kb *Cla*I–*Eco*RI exon 3 fragment) and GAPDH probes were labelled by the random primer method ('prime a gene system', Promega Co.). Autoradiographic signals were quantitated by using the Image 1.44 program to analyze autoradiograms scanned at 1200 d.p.i. with a UMAX scanner (Vista-S6).

Mapping of the 3′ c-*myc* mRNA UTR

Oligonucleotide/RNase H treatment. c-*myc* mRNA was annealed to a specific DNA oligonucleotide and treated with RNase H. Each specific oligonucleotide is complementary to the regions 7199–7218 (oligo 1) and 7257–7278 (oligo 2). Deoxyoligonucleotide sequences were CCTTACGCACAAAGAGTTCCG (oligo 1) and CAAGTTCATAGGTGATTGCTC (oligo 2). RNase H mapping was performed as described by Brewer and Ross (26) i.e. 40 µg total RNA were ethanol precipitated, resuspended in 20 µl 1 mM EDTA, pH 7.4, and heated at 70°C for 10 min. Oligonucleotide (0.5 µg) was added, and the reaction mixture was incubated at 20°C for 15 min. One µl of 4 M KCl was added and the mixture was incubated at 20°C for 15 min, followed by the addition of 20 µl TM buffer (40 mM Tris–HCl, pH 7.5, 60 mM $MgCl_2$). RNase H was added (final concentration 20 U/ml) and the digestion was performed at 37°C for 30 min. Following digestion, RNA was ethanol precipitated.

High resolution Northern blotting. RNA samples were separated by size, using a denaturing 4% polyacrylamide–urea gel as described by Stoeckle and Guan (25) and transferred electrophoretically to a charged mebrane (Zetaprobe, BioRad) according to the manufacturer's instructions. Filters were hybridized with the end-labelled deoxyoligonucleotide GGCTAAATCTTTCAGTCTCAAGACTCAGCCAAGGTTAGGTT which is complementary to the sequence 7300–7345.

Detection of 3′ c-*myc* mRNA fragments

Total RNA was isolated from HeLa 1C5 cells exposed to IFN-α before the induction with dexamethasone as previously described. Polyadenylated mRNA was isolated using the Oligotex mRNA kit from Qiagen. The isolated mRNA was digested with RNase H in the presence of oligo dT as described before and electrophoresed in 4% acrylamide–urea gel. The RNA was electrophoretically transferred to Zetaprobe membrane. c-*myc* sequences were identified using an antisense RNA probe transcribed *in vitro* with SP6 RNA polymerase, using the Riboprobe System SP6/T7 (Promega). The template for the reaction was the plasmid pEP 40 (26) digested with *Hin*dIII. Hybridization was carried out according to the directions supplied by the manufacturer using 1.5×10^6 c.p.m./ml and the final wash was performed with 0.1× SSC, 0.5% SDS at 60°C for 60 min.

Materials

IFN-α2β (INTRON-A) was obtained from Scherring Co., dexamethasone (Decadron) from Merck Co. Inc., RNase H from Gibco BRL, actinomycin D, cycloheximide and cordycepin from Sigma Chemical Co., and the deoxyoligonucleotides used in this study were synthesized by the Microchemistry Laboratory, Molecular Biology and Biotechnology Institute, Heraclion, Crete. The pEP 40 plasmid was a kind gift from Dr Ite Laird-Offringa.

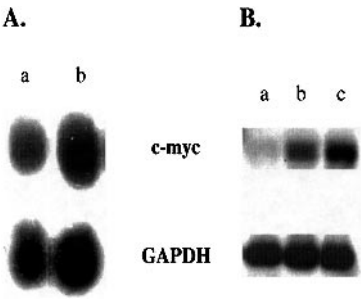

Figure 2. Effect of exposure to IFN-α on c-*myc* mRNA levels. (**A**) HeLa 1C5 cells were treated as described in Materials and Methods before addition 10% FCS + 10^{-5} M DX for 1 h. Lane a, control cells; lane b, cells exposed to 200 U/ml IFN-α for 24 h before the induction. (**B**) A pool of transfected cells was divided in three and maintained in culture as described in Materials and Methods. Cells were induced with 10% FCS (lane a), 10% FCS + 10^{-7} M DX (lane b) or 10% FCS + 10^{-7} M DX (lane c) after exposure for 24 h to 200 U/ml of IFN-α. Exposure to IFN-α before induction results in an ~2-fold increase in the c-*myc* mRNA levels in transfected cells.

RESULTS

Establishment and characterization of the HeLa 1C5 cell line

The study of the c-*myc* mRNA degradation pathways was approached by using a system in which high levels of c-*myc* mRNA expression could be attained and in which the rates of degradation of this mRNA could be modulated. High levels of steady state c-*myc* mRNA expression were achieved by adding dexamethasone to HeLa cells transfected with the eukaryotic expression vector pMSG, carrying c-*myc* sequences from –353 relative to P1 promoter to +500 3′ of the second polyadenylation site. On the other hand, addition of dexamethasone to the parental cell line HeLa resulted in the downregulation of c-*myc* mRNA (Fig. 1B). Since the SV40 polyadenylation signal of the vector was removed, the 3′ end of the induced c-*myc* mRNA was identical to that of the endogenous normal c-*myc* mRNA.

Out of several clones isolated after cotransfection with pSV2-neo only one stable clone, HeLa 1C5, was found to contain intact exogenous copies of the c-*myc* gene. A single *Eco*RI fragment (Fig. 1A) was found to hybridize to both c-*myc* 3′ sequences and the MMTV-LTR (data not shown). HeLa 1C5 cells were continuously maintained in the presence of 300 µg/ml G418. A year after the initial isolation the stability of the inserted sequences was confirmed by Southern blotting. Since transfected HeLa cells with pMSG-*myc* were gradually lost by apoptosis, the survival and the stability of HeLa 1C5 was attributed to the presence of a rearranged bcl-2 gene and to the expression of bcl-2 mRNA, which were detected (data not shown) (27). RNase H mapping of the 5′ end of the c-*myc* mRNA induced by dexamethasone in HeLa 1C5 cells, revealed that promoter usage was identical to that of untransfected cells (data not shown). No message initiating at the MMTV-LTR promoter could be detected. This observation can be explained on the basis of previous data that a functional P2 promoter prevents transcriptional read through from upstream promoters (28).

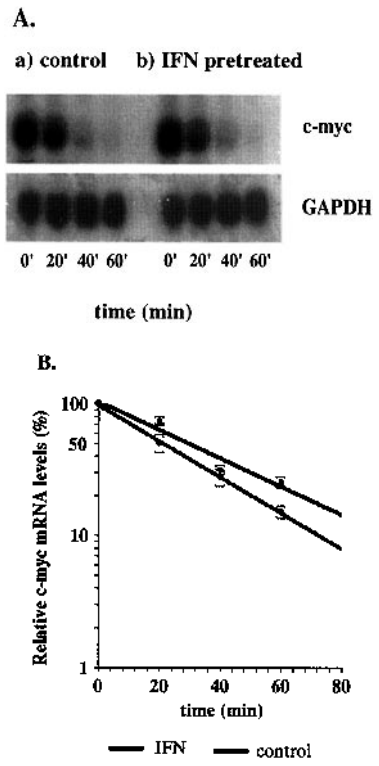

Figure 3. (A) Northern blot analysis of c-*myc* mRNA from HeLa 1C5 cells after actinomycin D chase. Cells were treated as described under Materials and Methods before the addition of 10% FCS + 10^{-5} M DX. Three hours later, actinomycin D (5 µg/ml final concentration) was added and RNA was isolated at the times indicated. (a) Control cells; (b) cells exposed to 200 U/ml IFN-α for 24 h. (**B**) Graphic representation of the results obtained by Northern blot analysis after normalization to the levels of GAPDH expression. Values are the mean of three experiments. Standard deviation is indicated by error bars. These data demonstrate that exposure to IFN-α results in a small albeit reproducible acceleration by 1.5× in the decay rate of c-*myc* mRNA.

Effects of IFN-α upon c-*myc* expression in HeLa 1C5 cells

We used IFN-α to test whether we could modulate c-*myc* mRNA stability in HeLa 1C5 cells. Exposure of HeLa 1C5 cells to IFN-α before dexamethasone induction resulted in a 2-fold increase in the steady state c-*myc* mRNA levels over the untreated cells, a finding also observed in the pools of transfected cells (Fig. 2) in contrast with what has been reported for the parental cell line (29), and in agreement with the effect observed in other cell lines such as HL-60 and U-937 (30). However, despite the increase, actinomycin D chase revealed that c-*myc* mRNA decays more rapidly in HeLa 1C5 cells exposed to IFN-α (Fig. 3). Therefore, the 2-fold increase in the levels of c-*myc* mRNA expression could not be attributed to stabilization since the c-*myc* mRNA isolated from cells exposed to IFN-α was relatively less stable (~1.5×) than that of the control cells. The observed effect of IFN-α upon c-*myc* mRNA stability in HeLa 1C5 cells was reproducible and was comparable with that observed in other cell lines (31,32). Thus, this system, which could provide high levels of rapidly degraded c-*myc* mRNA, was suitable for the investigation of the degradation mechanism of this mRNA and the identification of intermediate products.

Detection of c-*myc* mRNA truncated fragments

Previous data indicate that exposure of cells to IFN-α results in the reduction of the cytoplasmic poly(A) polymerase activity (33). These observations and the increased instability of the c-*myc* mRNA in these cells led us to investigate whether any alterations in the length of the poly(A) tail were caused by IFN-α which resulted in faster decay (34). In order to test whether the IFN-α action is exerted through alterations in the poly(A) status or alterations in the rate of deadenylation or by an alternative mechanism, we proceeded in RNase H mapping of the 3′ end of c-*myc* mRNA as described in Materials and Methods. Figure 4 shows the sequences recognized by the oligonucleotides used in this study in the RNAse H reactions and the oligonucleotide used as the probe to detect the reaction products. This experimental approach was expected to yield RNA fragments extending above 269 and 411 nt derived from pA1 and pA2 polyadenylation signals respectively when oligonucleotide 2 was used, and fragments extending over 329 and 471 when oligonucleotide 1 was used (35). Since pA2 is the major polyadenylation signal (26) we expected that the majority of the reaction products would range from 411 to ~600 nt or from 471 to 670 nt depending on the oligonucleotide used in the reaction.

Figure 5 includes the data obtained from RNase H mapping using oligo 2 of RNA isolated from HeLa 1C5 cells under various conditions of c-*myc* mRNA induction. The following observations were made. (i) Under all conditions tested the c-*myc* mRNA polyadenylated at the pA2 site did not have a homogeneous distribution in the lengths of poly(A) tails. A significant proportion of the message had short or no poly(A) tails and this became more evident under conditions of c-*myc* mRNA overexpression. (ii) The densitometric scans of autoradiograms indicated that exposure to IFN-α did not have a drastic effect upon poly(A) tail sizes (Figs 5B and 3). (iii) In addition to the full length polyadenylated c-*myc* mRNA at the two polyadenylation sites, we observed a specific pattern of smaller products in all RNA samples (fragments I, II and III). These three smaller species were more prominent and had an altered internal distribution in mRNA from cells exposed to IFN-α (Fig. 5C). In lane 4 the data from RNA isolated from cells treated with the polyadenylation inhibitor cordycepin are shown. The adenosine analogue cordycepin (3′dA) which mainly interferes in the formation of the poly(A) tail by preventing chain elongation (36) alters the distribution of the poly(A) tails of intact c-*myc* mRNA, synthesized in its presence, towards smaller sizes. Cordycepin addition did not have any effect on the appearance of the smaller species and furthermore, no change in the mobility of the truncated species was observed suggesting that they do not possess poly(A) tails. The absence of poly (A) tails was confirmed by the fact that the mobility of the truncated fragments was not altered after removal of the poly(A) tails with RNase H in the presence of oligo dT (data not shown).

When using a second oligo which recognizes sequences 60 nt downstream, the size of the smaller bands shifted accordingly, indicating that these were derived from truncated c-*myc* mRNA generated *in vivo*. The appearance of these specific intermediate products was dependent on the presence in the reaction of RNase H and an oligonucleotide (Fig. 6; lanes 3 and 4 share the same non-specific background). The estimated sizes of the fragments place the 3′ ends of the *in vivo* intermediate products at the regions presented in Figure 6B. The existence of identical in size minor products was also confirmed in the untrasfected HeLa cells (Fig. 7).

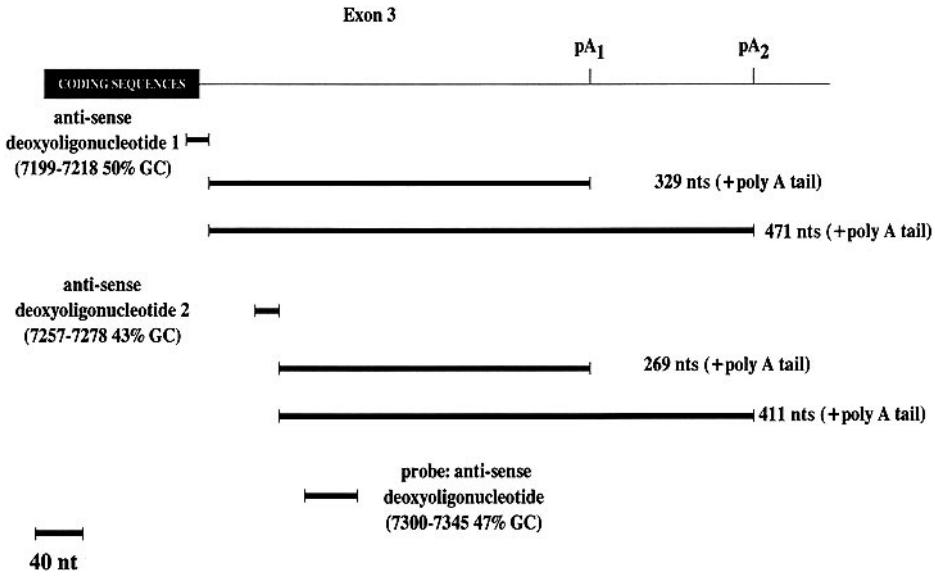

Figure 4. Schematic representation of the 3′ UTR of the c-*myc* mRNA showing the positions of the sequences recognized by oligo 1 and oligo 2 used for RNase H mapping, the expected fragments and the position of the oligo used as probe.

The intensity of the three major bands correlated with the levels of c-*myc* mRNA expression characteristic of the two cell lines, HeLa 1C5 induced with dexamethasone and HeLa (lanes 1 and 2).

The truncated c-*myc* mRNAs which we detect, could possibly represent the products of the process following the deadenylation step and they could be generated either via endonucleolytic cleavage or they became detectable due to defined pausing of an exonuclease. Alternatively, they could be generated by the activation of an independent degradation mechanism involving endonucleolytic cleavage.

The last hypothesis would predict the existence of matching 3′ end fragments for the truncated intermediates of c-*myc* mRNA. In order to identify such intermediates, polyadenylated mRNA was isolated from HeLa 1C5 cells cultured under conditions in which the truncated species were most prominent, i.e., exposure to IFN-α before induction with dexamethasone. The poly(A) tails were removed by digestion with RNase H in the presence of oligo dT and the RNA was analyzed by high resolution Northern blotting. The 3′ end c-*myc* mRNA sequences were recognized using a radioabeled antisense RNA probe transcribed *in vitro* which spans the 3′ UTR and recognizes the last 369 nt (26). Under the conditions employed, any fragment detected other than the full length c-*myc* mRNA must represent 3′ c-*myc* mRNA sequences which retain a minimal poly(A) tail, at least. The results shown in Figure 8 demonstrate apart from the full length c-*myc* mRNA several such distinct fragments. Among those, E, D and C could represent the matching fragments for the truncated species I, II and III (Fig. 5) respectively. The existence of longer fragments is also evident. The identification of the truncated intermediates I, II and III and the detection of adenylated 3′ truncated fragments (Fig. 8) suggest that c-*myc* mRNA may be subjected *in vivo* to endonucleolytic cleavage.

It could be postulated that the process generating the above degradation intermediates is a subsequent step to the deadenylation process therefore, a precursor–product relationship should exist between the oligoadenylated c-*myc* mRNA and the truncated products. This would lead to the prediction that, as long as precursor RNA is available, the truncated species would be generated at a steady rate. To investigate the above possibilities we performed an actinomycin D chase under various conditions and we proceeded to RNase H mapping of the c-*myc* mRNA. The data in Figure 9 show that under all conditions applied (i.e., induction with serum or exposure to IFN-α before the induction) there was a gradual deadenylation process and accumulation of c-*myc* mRNA species having short poly(A) tails. The accumulation of short tailed c-*myc* mRNA did not result in the enhancement of the truncated products. On the contrary, the intensity of these products was reduced as the chase proceeded even though the intact oligoadenylated form persisted (Fig. 9c and d). Thus, c-*myc* mRNA degraded through sequential deadenylation did not appear to be a precursor to the truncated species unless the process of their generation was inhibited by actinomycin D. There was, also, no indication that any of the truncated species was a precursor to a shorter one. The above observations may suggest that the truncated species are generated by an alternative endonucleolytic degradation mechanism which may not require deadenylation.

Our data are compatible with the existence of a degradation mechanism of c-*myc* mRNA resulting in the generation of truncated intermediates, probably through endonucleolytic cleavage at several sites. The enhanced presence of these truncated products in cells exposed to IFN-α may suggest the further activation of this mechanism.

DISCUSSION

The study of the regulation of mRNA stability has been approached in several ways. For unstable mRNAs, such as those of oncogenes, cytokines etc., in which rapid decay is a critical regulatory step of gene expression, the focus has been on *cis*-acting elements conferring instability, *trans*-acting factors controlling degradation and the sequence of events in the process of degradation. It is known that the half-life of certain mRNAs, such as that of c-*myc*, can be modulated by physiological stimuli. The elucidation of the changes in the mechanism of degradation

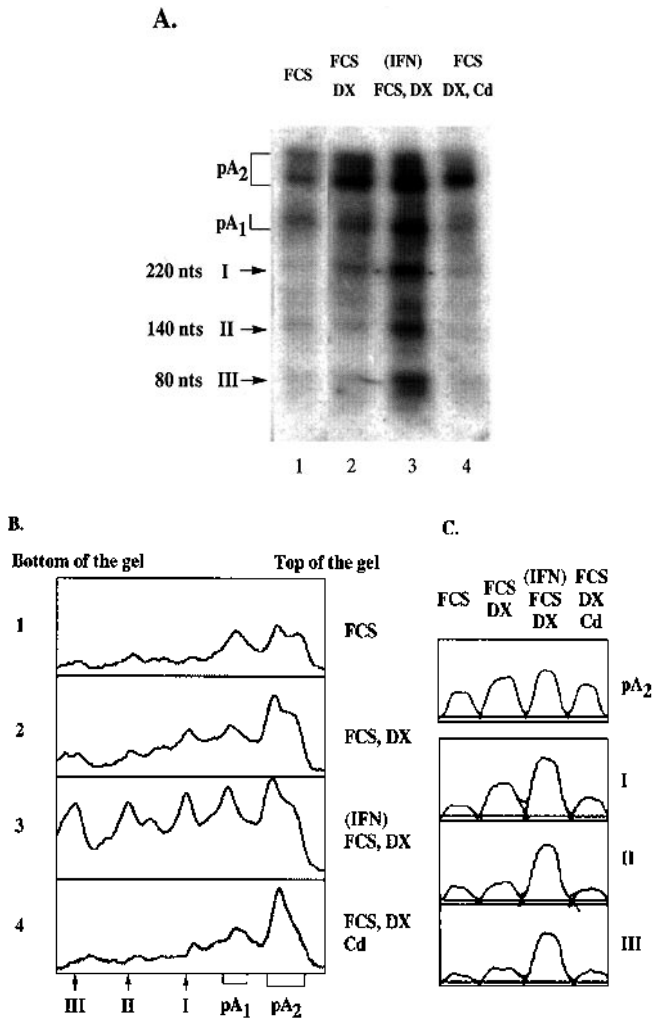

Figure 5. RNase H mapping of the c-*myc* mRNA in HeLa 1C5 cells reveals a non-uniform distribution in the sizes of the poly(A) tails and the existence of truncated c-*myc* mRNA species. (**A**) HeLa 1C5 cells were treated as described in Materials and Methods before addition of 10% FCS (lane 1); 10% FCS + 10^{-5} M DX (lane 2); 10% FCS + 10^{-5} M DX after exposure to 200 U/ml IFN-α for 24 h (lane 3); 10% FCS + 10^{-5} M DX in the presence of 20 µg/ml cordycepin (Cd) (lane 4). RNA was isolated 3 h later and RNase H mapping was performed as described under Materials and Methods, using oligo 2 for the cleavage reaction. The brackets show the distribution of the polyadenylated fragments derived from pA2 and pA1 polyadenylation sites. The arrows indicate the position of the minor fragments I, II and III and their estimated sizes. (**B**) Densitometric scans of the corresponding lanes. Scan of lane 4 shows that cordycepin resulted in a shift towards smaller sizes of poly(A) tails and that the oligoadenylated species mainly present were producing a peak. The same identifiable peak is present in the other lanes indicating an enhanced representation of oligoadenylated species. The c-*myc* mRNA species with longer poly(A) tails have a uniform distribution in lanes 1, 2 and 3. (**C**) Densitometric scans of the different distinct products across the lanes show the proportional relation between intact c-*myc* mRNA and truncated species under the conditions tested. Exposure to IFN-α caused a marked increase in the intensity of the smaller fragments with respect to the intact c-*myc* mRNA, while cordycepin did not have any noticeable effect.

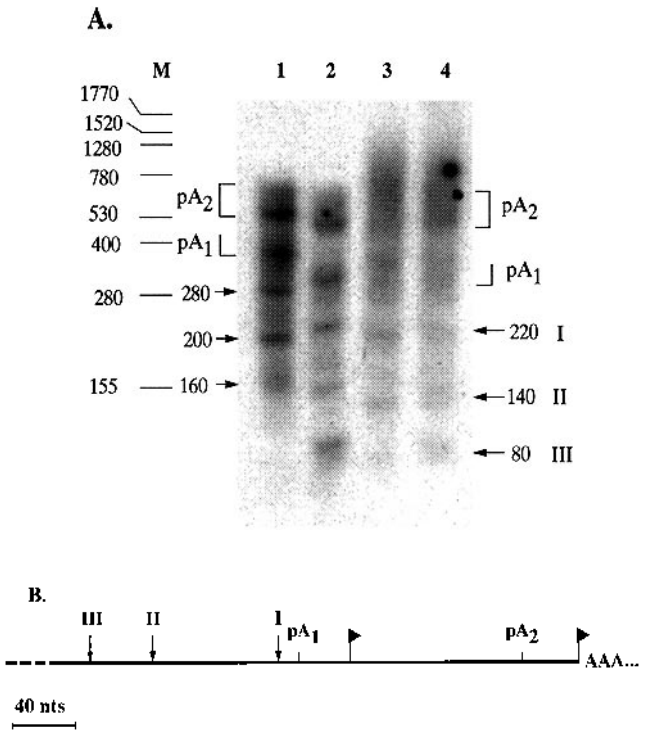

Figure 6. Characterization of c-*myc* mRNA truncated species. (**A**) RNase H mapping of c-*myc* mRNA from HeLa 1C5 cells exposed for 3 h to 10% FCS + 10^{-5} M DX using oligo 1 (lane 1); oligo 2 (lane 2); no oligo (lane 3); no RNase H (lane 4). M: RNA markers. The arrows on the left of the figure indicate the position and the estimated sizes of the minor products generated with oligo 1 (lane 1). Correspondingly, the arrows on the right of the figure indicate the positions and the sizes of the smaller products when using oligo 2 (lane 2). Accordingly the brackets show the distribution of the poly(A) tails derived form pA2 and pA1. (**B**) Relative positions of the cleavage regions on the 3′ end of the c-*myc* mRNA. The flags indicate the positions where polyadenylation starts following the polyadenylation signals pA1 and pA2. The arrows indicate the positions of the corresponding sites.

under the influence of such physiological stimuli will help identify the key steps in mRNA decay and the factors affecting mRNA stability.

Removal of the poly(A) tail seems to be a prerequisite step in the degradation process of the majority of mRNAs. Differences in the stability of mRNAs are attributed to the differences in the rate of deadenylation. Since in stable mRNAs, such as globin mRNA, deadenylation stops upon reaching a minimum length of poly(A) protecting the message from exonucleolytic attack, it is believed that the instability elements present in unstable mRNAs act by enhancing the rate of deadenylation and further by promoting the complete removal of poly(A) tail (11,34,37). Therefore, for unstable mRNAs it is proposed that the rate of deadenylation is the critical step of degradation. For example, Laird-Offringa *et al.* (38) have shown that c-*myc* mRNA from HeLa cells is rapidly deadenylated before final degradation and have proposed that deadenylation is the rate limiting step *in vivo*. Studies using an *in vitro* decay system provide similar evidence (39). Shyu *et al.* (40) have shown that AREs from the c-*fos* mRNA mediate decay by first stimulating deadenylation and then by providing an element that directs the next phase of the degradation process. Nevertheless, uncoupling of the two elements was achieved by point mutations that maintained the ability to control deadenylation but abolished the ability to stimulate further decay. This observation indicates that the decay of unstable mRNAs may also involve a two step process.

Assuming that the deadenylation process of c-*myc* mRNA occurs at a steady rate—at all its stages—and when the mRNA

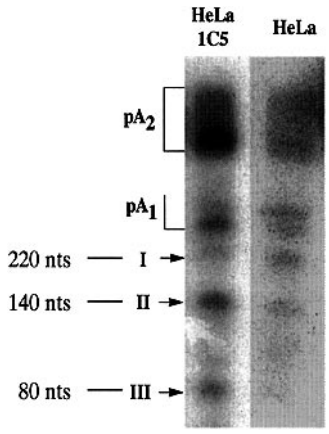

Figure 7. RNase H mapping (using oligo 2) of c-*myc* mRNA isolated from HeLa 1C5 induced with 10% FCS + 10^{-5} M DX (left lane) or HeLa cells induced with 10% FCS (right lane). The arrows show the position of the smaller products. Note that their intensity correlates with total steady state c-*myc* mRNA levels.

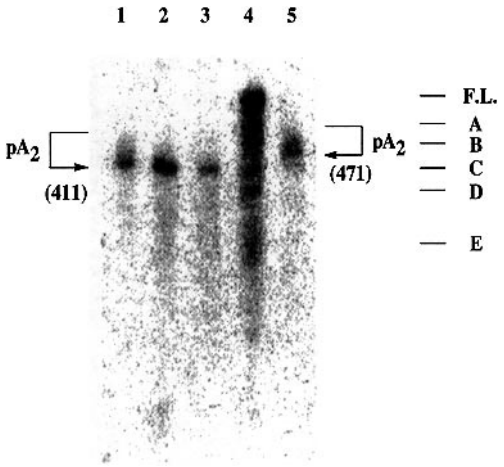

Figure 8. Identification of adenylated c-*myc* mRNA fragments lacking 5′ sequences. The following RNA samples were analyzed by high resolution Northern blotting using ^{32}P-labelled antisense RNA spanning the 3′ UTR c-*myc* sequences (see Materials and Methods). Lane 1, 60 µg total RNA was digested with RNase H in the presence of oligo 2; lane 2, as in lane 1, in the presence of oligo dT; lane 3, 70 µg polyA(–) RNA was treated as in lane 1; lane 4, poly (A)+ mRNA isolated from 400 µg total RNA was digested with RNase H in the presence of oligo dT; lane 5, 60 µg total RNA was digested with RNase H in the presence of oligo 1. Brackets show the distribution of poly(A) tails derived from pA2 and arrows point out the position of the deadenylated fragments derived from cleavage with RNase H in the presence of oligo 2 (left) or oligo 1 (right). The size of the deadenylated fragments is noted in the parenthesis. Removal of the poly(A) tails from poly(A)+ mRNA revealed in addition to full length c-*myc* mRNA five smaller bands. The letters A, B, C, D and E on the right indicate the position of the distinct c-*myc* mRNA fragments and F.L. the position of the full length c-*myc* mRNA.

becomes deadenylated it rapidly decays, then one would expect that all sizes of poly(A) tail should be equally represented at any time during this process. The data presented here show that in HeLa 1C5 cells there was no homogeneous distribution in the size of poly(A) tails. We observed an accumulation of c-*myc* mRNA with short or no poly(A) tails. Our experimental approach does not allow the distinction between oligoadenylated or completely deadenylated mRNA. We consider likely that it is oligoadenylated, based on the observations of Chen and Shyu (41) who show that deadenylation of chimeric mRNAs carrying the 3′ UTR of c-*myc* does not lead to complete removal of the poly(A) tail. The data in Figure 9 show that the oligoadenylated c-*myc* mRNA species was derived by the deadenylation process and was more stable than its precursor.

Swartwout and Kinninburgh (10) have estimated that non-adenylated mRNA is more stable in HL-60 cells since the half-life for poly(A)-c-*myc* mRNA is twice as long as that for poly(A)$^+$. Furthermore, Chen and Shyu (41) suggest that the time required for deadenylation is much shorter than the time required for the overall decay. All the above observations indicate that the metabolic fate of the oligoadenylated message determines the decay rate of c-*myc* mRNA, provided that it reaches the oligoadenylated state.

RNase H mapping revealed the presence of smaller non-adenylated fragments hybridizing to c-*myc* 3′ end sequences. These fragments did not represent small RNAs crossreacting with the probe, since they were absent when no RNase H or oligonucleotides were used in the reaction (Fig. 6). When using two different oligonucleotides which recognized sequences 60 nt apart, the products yielded by RNase H digestion showed a corresponding shift in size. This observation also excluded the possibility of inaccurate cleavage due to non-specific RNA–oligonucleotide hybrid formation. Furthermore, the internal distribution of these fragments was altered in response to IFN-α (Fig. 5). Thus, we concluded that they represented truncated c-*myc* mRNAs generated *in vivo*.

The presence of these intermediates which we observed can be accounted in two ways: such fragments may result through endonucleolytic cleavage or due to a defined pause in the processive action of a 3′–5′-exonuclease. The identification of adenylated fragments containing c-*myc* mRNA 3′ sequences support the former hypothesis. The putative endonucleolytic cleavage could either follow the deadenylation process as it has been reported for human gro-α mRNA (42) or could occur due to the activation of an alternative degradation mechanism, independent of deadenylation. Such intermediates have been reported before. A short form of the TfR mRNA has been identified lacking at least a portion of 3′ UTR (43). Truncated mRNAs have been reported for other eukaryotic mRNAs as well, including chick fibroblast 9E3 (44), chicken apo VLDL II (45), *Xenopus* Xlhbox 2b (46) and human histone H4 (35). For some of the above truncated mRNAs matching adenylated fragments have been identified which would prove the existence of an alternative degradation mechanism involving endonucleolytic cleavage. These include chicken liver apo VLDL mRNA, *Xenopus* oocyte Xlhbox 2b mRNA, chick fibroblast 9E3 mRNA, mouse albumin mRNA (47) and TfR mRNA(43).

A truncated mRNA encoding for c-*myc* has been observed before but was not identified as such (26). Brewer and Ross (39) have reported the *in vitro* generation of truncated c-*myc* mRNA species following the deadenylation process which derive from mRNA adenylated at the pA2 site and terminate between pA1 and pA2. These are not related to the three species of truncated c-*myc* mRNAs which we identified since they have different sizes and they arise through a different mechanism. Our experimental approach would not permit us to distinguish products terminating between pA1 and pA2 from the message adenylated at the pA1 site. The truncated products which we identified seem to arise

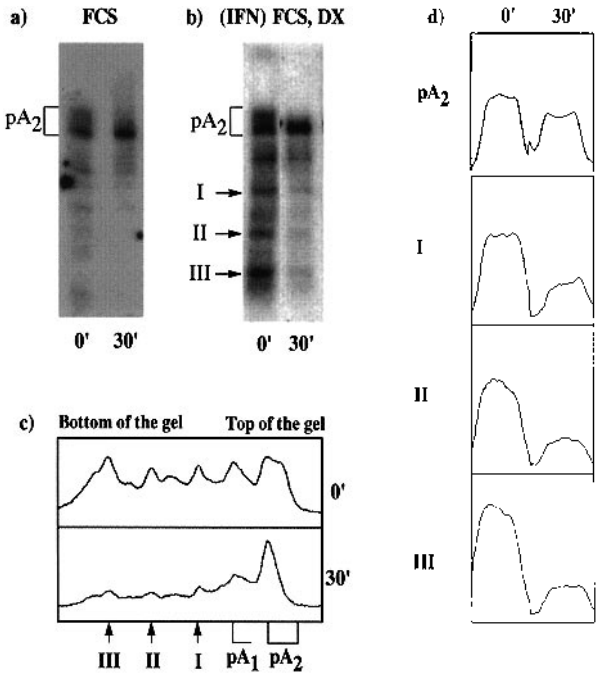

Figure 9. RNase H mapping of c-*myc* mRNA isolated after actinomycin D chase from cells treated with (**a**) 10% FCS and (**b**) 10% FCS + 10^{-5} M DX after exposure to 200 U/ml IFN-α for 24 h. Actinomycin D (final concentration 5 μg/ml) was added 3 h later and RNA was isolated at the times indicated. Densitometric scans of the corresponding lanes in b (**c**) and across the lanes in b (**d**) show that the truncated species decay rapidly and that they do not appear to be generated from the oligoadenylated species derived through deadenylation.

through a process independent of deadenylation from poly(A)(+) c-*myc* mRNA species. When analyzing the poly(A)(+) RNA we identified several c-*myc* mRNA fragments lacking 5′ sequences. Three of them are candidates for the matching fragments of the truncated species. The existence of larger fragments implies the existence of additional cleavage sites 5′ to the sequences which we studied and which spans the last 471 nt of c-*myc* mRNA.

Endonucleolytic cleavage of c-*myc* mRNA has been demonstrated within a sequence further upstream to the area we studied. Endonucleolytic cleavage was attained by competing out, *in vitro*, a protective 70 kDa protein which binds to the 180 nt instability element in the coding region (48). Evidence for multiple endonucleolytic cleavage sites within the c-*myc* 3′ UTR has been also provided by *in vitro* studies in which these sequences were cleaved by a human RNase E-like enzyme (49).

The loss of polyadenylated c-*myc* mRNA without prior deadenylation has been reported before in HL-60 cells induced for differentiation (10). The truncated products which we identified also seem to arise independently from poly(A)(+) c-*myc* mRNA. We base this assumption on the actinomycin D data demonstrating that there is no obvious precursor–product relationship between poly(A)(–) c-*myc* mRNA and the truncated species (Fig. 9c and d), which indicates that the oligoadenylated message does not unconditionally become converted to truncated species. The truncated products disappear even though intact oligoadenylated c-*myc* mRNA is available (Fig. 9). This observation can be explained either by an alternative degradation mechanism which is independent of deadenylation or by the possibility that the mechanism generating truncated species is sensitive to actinomycin D. In that case the metabolic fate of deadenylated c-*myc* mRNA is controlled by more than one mechanisms only one of which is sensitive to this drug, since actinomycin D does not stabilize c-*myc* mRNA overall. The use of IFN-α in our system allowed us to conclude that the appearance of truncated c-*myc* mRNAs is regulated. IFN-α in HeLa 1C5 increased the steady state c-*myc* mRNA levels opposite to its effect upon HeLa cells (31). However, IFN-α maintained its destabilizing action since the rate of c-*myc* mRNA decay increased after exposure to IFN-α. RNase H mapping showed that the amounts of truncated species increased, as well. The question arises whether the enhanced endonucleolytic cleavage was a direct or indirect effect of IFN-α which occurred in response to high steady state levels of c-*myc* mRNA, as an emergency feedback mechanism, efficiently preventing translation of the surplus message.

A mechanism exists which is a likely candidate in mediating such an IFN-α induced action. IFNs induce 2′–5′ oligo(A)synthetase whose product, 2′–5′ oligo(A), activates in turn the latent endonuclease RNase L (50). The activation of RNase L may account for the enhanced endonucleolytic cleavage of c-*myc* mRNA. Partial abrogation of 2′–5′ oligo(A) synthetase activity reverses the destabilizing effect of IFN-α upon c-*myc* mRNA, indicating that IFN action may be mediated through RNase L (33). Alternatively, IFN-α could exert its effects either by releasing sequence specific RNA binding proteins which protect c-*myc* mRNA from endonucleolytic attack or by inducing the binding of destabilizing proteins. These mechanisms are not mutually exclusive.

Our system will provide the opportunity to address some of these questions. It would be of interest, for example, to investigate whether blocking the 2′–5′ oligo (A) synthetase pathway would inhibit the generation of c-*myc* mRNA truncated species. Precise mapping of the cleavage sites would confirm the mechanism of endonucleolytic cleavage and perhaps would provide information about the sequence specificity of this process.

ACKNOWLEDGEMENTS

The authors thank Drs J. Ross, M. S. Coleman and D. H. Sorscher for their critical comments on the manuscript, and Dr C.M. Tsiapalis for his suggestions. This work was supported by a grant from the Greek Ministry of Health to T.T. We would also like to thank the Greek Society for Cancer Study for financial support.

REFERENCES

1 Marcu,K.B., Bossone,S.A. and Patel,A.J. (1992) *Annu. Rev. Biochem.*, **61**, 809–860.
2 Spencer,C. and Groudine,M. (1991) *Adv. Cancer Res.* **56**, 1–50.
3 Evan,G.I., Wyllie,A.H., Gilbert,C.S., Littlewood,T.D., Land,H., Brooks,M., Waters,C.M., Penn,L.Z. and Hancock.,D.C. (1992) *Cell*, **69**, 111–122.
4 Shi,Y., Glynn,J.M., Guilbert,L.J., Cotter,T.G., Bissonette,R.P. and Green,D.E. (1992) *Science* **257**, 212–214.
5 Meichle,A., Philipp,A. and Eilers,M. (1992) *Biochim. Biophys. Acta.* **1144**, 129–146.
6 Dani,C., Blanchard,J.M., Piechaczyk,M., El Sabouti,S., Marty,L. and Jeanteur,P. (1984) *Proc. Natl. Acad. Sci. USA* **81**, 7046–7050.
7 Ramsay,G., Evan,G.I. and Bishop,J.M. (1984) *Proc. Natl. Acad Sci. USA* **81**, 7742–7749.
8 Blanchard,J.M., Piechaczyk,M., Dani,C., Chambard,J.C., Franchi,A., Pouyssegur,J. and Jeanteur,P. (1985) *Nature* **317**, 443–445
9 Mechti,P., Piechaczyk,M., Blanchard,J.M., Marty,L., Bonnieu,A., Jeanteur,P. and Lebleu,B. (1986) *Nucleic Acids Res.* **14**, 9653–9660.
10 Swartwout,S.G. and Kinninburgh,A.J. (1989) *Mol. Cell. Biol.* **9**, 288–295.

11 Schiavi,S.C., Belassco,J.G. and Greenberg,M.E. (1992) *Biochim. Biophys. Acta* **1114**, 95–106.
12 Shaw,G. and Kamen,R. (1986) *Cell* **46**, 659–667.
13 Jones,T.R. and Cole,M.D. (1987) *Mol. Cell. Biol.* **7**, 4513–4521.
14 Bonnie,A.P., Roux,P., Marty,L., Jeanteur,P. and Piechaczyk,M. (1990) *Oncogene* **5**, 1585–1588.
15 Alberta,J.A., Rundell,K. and Stiles,C.D. (1994) *J. Biol. Chem.* **269**, 4532–4538.
16 Brewer,G. (1991) *Mol. Cell. Biol.* **11**, 2460–2466.
17 Vakalopoulou,E., Shaack,J. and Shenk,T. (1991) *Mol. Cell. Biol.* **11**, 3355–3364.
18 Wisdom,R. and Lee,W. (1991) *Genes Dev.* **5**, 232–234.
19 Dani,C., Mechti,N., Piechaczyk,M., Lebleu,B., Jeanteur,P. and Blanchard,J.M. (1985) *Proc. Natl. Acad. Sci. USA* **82**, 4896–4899.
20 Knight,E., Anton,E.D., Fahey,D., Friedland,B.K. and Jonak,G.J. (1985) *Proc. Natl. Acad. Sci. USA* **82**, 1151–1154.
21 Gazin,C., Dupont de Dinechin,S., Hampe,A., Masson,J.M., Martin,P., Stehelin,D. and Galibert,F. (1984) *EMBO J.* **3**, 383–387.
22 Graham,F.L., Baccheti,S., McKinnon,R., Stanners,G., Cordell,B. and Goodman,H. (1980) in Baserga,R., Croce,C. and Rivera,G. (eds), *Introduction of Macromolecules into Viable Cells.* Alan R. Liss. NY. pp. 3–22.
23 Chomczynski,P. and Sacchi,N. (1987) *Anal. Biochem.* **162**, 156–159.
24 Brewer,G. and Ross,J. (1990) *Methods Enzymol.* **181**, 202–209.
25 Stoeckle,M.Y. and Guan,L. (1993) *BioTechniques* **15**, 230–231.
26 Laird-Offringa,I.A., Elfferich,P., Knaken,H.J., de Ruiter,J. and van der Eb,A.J. (1989) *Nucleic Acids Res.* **17**, 6499–6514.
27 Bissonette,R.P., Echeverri,F., Mahboubi,A. and Green,D.R. (1992) *Nature* **359**, 552–556.
28 Strobl,L.J., Kohlhuber,F., Mautner,J., Polack,A. and Eick,D. (1993) *Oncogene* **8**, 1437–1447.
29 Kelly,J.M., Gilbert,C.S., Stark,G.R. and Kerr,I.M. (1985) *Eur. J. Biochem.* **153**, 367–371.
30 Kimchi,A. (1987) *Interferon* **8**, 85–110.
31 Chatterjee,D. and Savarese,T.M. (1992) *Cancer Chemother. Pharmacol.* **30**, 12–20.
32 Meurs,E. and Hovanessian,A.G. (1988) *EMBO, J.* **7**, 1689–1696.
33 Havredaki,M., Garyfallides,S. and Tsiapalis,C.M. (1992) *J. Biol. Regulators and Homeostatic Agents* **6**, 143–144.
34 Sachs,A.B. (1993) *Cell*, **74**, 413–421.
35 Ross,J., Peltz,S.W., Kobs,G. and Brewer,G. (1986) *Mol. Cell. Biol.* **6**, 4362–4371.
36 Shuman,S. and Moss,B. (1988) *J. Biol. Chem.* **263**, 8405–8412.
37 Laird-Offringa,I.A. (1992) *BioEssays*, **14**, 119–124.
38 Laird-Offringa,I.A., De-Wit,C.L., Elfferinch,P. and Van Der Eb,A.J. (1990) *Mol. Cell. Biol.* **10**, 6132–6140.
39 Brewer,G. and Ross,J. (1988) *Mol. Cell. Biol.* **8**, 1697–1708.
40 Shyu,A.B., Belasco,J.G. and Greenberg,M.E. (1991) *Genes Dev.* **5**, 221–231.
41 Chen,C.-Y. and Shyu,A.-B. (1994) *Mol. Cell. Biol.* **14**, 8471–8482.
42 Stoeckle,M.Y. (1992) *Nucleic Acids Res.* **20**, 1123–1127.
43 Binder,R., Horowitz,A.J., Basilion,J.P., Koeller,D.M., Klausner,R.D. and Harford,J.B. (1994) *EMBO J.* **13**, 1969–1980.
44 Stoeckle,M. and Hanafusa,H. (1989) *Mol. Cell. Biol.* **9**, 4738–4745.
45 Binder,R., Hwang,S.L., Ratnasabapathy,R. and Williams,D.L. (1989) *J. Biol. Chem.* **264**, 16910–16918.
46 Brown,B.D. and Harland,R.M. (1990) *Genes Dev.* **4**, 1125–1135.
47 Tharun,S. and Sidershmukh,R. (1995) *Nucleic Acids Res.* **23**, 641–646.
48 Bernstein,P.L., Herrick,D.J., Prockipcak,R.D. and Ross,J. (1992) *Genes Dev.* **6**, 642–654.
49 Wennborg,A., Sohlberg,B., Angerer,D., Klein,G. and von Gabain,A. (1995) *Proc. Natl. Acad Sci. USA* **92**, 7322–7326.
50 Kerr,I.M. (1987) *J. Interferon Res.* **7**, 505–510.